SCIENTIFIC REPORTS

OPEN

SUBJECT AREAS:
ANTIMICROBIALS
ENZYMES
MICROBIOLOGY
STRUCTURAL BIOLOGY

Received
12 May 2011

Accepted
28 July 2011

Published
12 August 2011

Correspondence and requests for materials should be addressed to E.S. (e.sim@kingston.ac.uk)

Activation of nitrofurazone by azoreductases: multiple activities in one enzyme

Ali Ryan[1,2], Elise Kaplan[1], Nicola Laurieri[1], Edward Lowe[3] & Edith Sim[1,2]

[1]Pharmacology Department, University of Oxford, OX1 3QT, [2]Faculty of Science, Engineering and Computing, Kingston University, KT1 2EE, [3]Laboratory of Molecular Biophysics, Biochemistry Department, University of Oxford, OX1 3QU.

Azoreductases are well known for azo pro-drug activation by gut flora. We show that azoreductases have a wider role in drug metabolism than previously thought as they can also reduce and hence activate nitrofurazone. Nitrofurazone, a nitroaromatic drug, is a broad spectrum antibiotic which has until now been considered as activated in bacteria by nitroreductases. The structure of the azoreductase with nitrofurazone bound was solved at 2.08 Å and shows nitrofurazone in an active conformation. Based on the structural information, the kinetics and stoichiometry of nitrofurazone reduction by azoreductase from *P. aeruginosa*, we propose a mechanism of activation which accounts for the ability of azoreductases to reduce both azo and nitroaromatic drugs. This mode of activation can explain the cytotoxic side-effects of nitrofurazone through human azoreductase homologues.

Azoreductases are a group of NAD(P)H dependent flavoenzymes that have been identified in a range of bacterial species found in the gut including *E. coli*[1] and *P. aeruginosa*.[2] Members of this family are also found in humans where they are known as NAD(P)H quinone oxidoreductases.[3] The importance of azoreductases in drug metabolism in the gut is well known for azo drugs used to treat inflammatory bowel disease *e.g.* balsalazide.[4] Data have shown that these enzymes can reduce a number of other classes of substrate including, quinones[1, 5] and nitroaromatics.[6] As a result of the diverse substrate specificity profile it is suggested that the role of azoreductases in drug metabolism may be wider than originally thought.

Nitroaromatic groups are found in a range of drugs currently on the market including the anti-inflammatory nimuselide and the parkinson's disease treatment tolcapone. A common feature of some nitroaromatic drugs is hepatotoxicity resulting from reduction of the nitro group.[7] Nitrofurazone was selected as an example of a nitroaromatic drug to study the mechanism of nitroreduction by azoreductases and their human homologues NAD(P)H quinone oxidoreductases. Nitrofurazone (Fig. 1) is a topical antibiotic mainly used to treat burns and skin grafts. Nitrofurazone is part of the 5-nitrofuran family, which are potent antibiotics, active against both Gram-positive and Gram-negative bacteria. Members of the 5-nitrofuran family are being developed as therapies for multidrug resistant bacteria e.g. *M. tuberculosis*.[8] Nitrofurazone and the other members of this family have a common mode of action that requires intracellular activation by nitroreductases. As a result, mutations within two nitroreductases known as nitrofuran sensitivity genes A and B (NfsA and B) from *E. coli* provide nitrofurazone resistance.[9] As humans lack nitroreductases such as these, the majority of nitroreduction will be carried out by NAD(P)H quinone oxidoreductases.[10] Activation by nitroreductases results in four electron reduction of the nitro group to a reactive hydroxylamine metabolite[11] that in combination with the nitroso oxidation product causes DNA damage.[12]

Three azoreductases from *P. aeruginosa*, paAzoR1, paAzoR2 and paAzoR3, have been extensively characterised.[2, 5, 13, 14] A recent structural study has provided insight into the mechanism by which azoreductases activate azo drugs, and also explains their ability to reduce both azo and quinone substrates.[13] The aforementioned ability of azoreductases to act as nitroreductases indicates they may also reduce nitrofurazone.[6, 15]

The structure of *E. coli* NfsB bound to nitrofurazone has been solved[11] the structure showed nitrofurazone bound in what the authors described as an inactive conformation within the enzyme active site. In order for their proposed mechanism of reduction to be correct nitrofurazone has to reverse its binding orientation as a result of FMN being in the reduced state. The work described in this manuscript demonstrates that azoreductases can also reduce nitrofurazone and describes the kinetics of nitrofurazone reduction by paAzoR1 as well as the structure of nitrofurazone bound to paAzoR1 in an active conformation. Based on this structure, a putative mechanism is

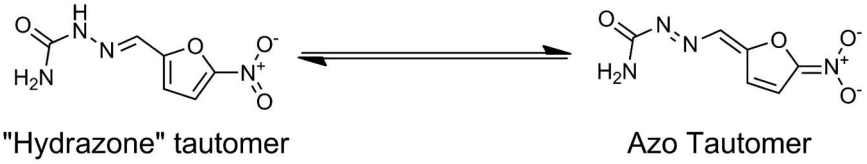

Figure 1 | Structure of nitrofurazone. Figure showing the two nitrofurazone tautomers that occur in equilibrium in solution.

proposed for the reduction of nitrofurazone by azoreductases that is also applicable to the mechanism of reduction of nitrofurazone and other nitroaromatic drugs by bacterial azoreductases and by their human homologues.

Results

Nitrofurazone is reduced by paAzoR1. Nitrofurazone was shown to be reduced by paAzoR1, apparent K_m and V_{max} values were obtained via Lineweaver-Burk plots. The apparent K_m for paAzoR1 was 15.7 ± 1.6 μM and the V_{max} was 9.8 ± 0.6 μM.s^{-1}.mg of enzyme^{-1}. Via equations (1) and (2) the rates of nitrofurazone reduction and NADPH oxidation were obtained simultaneously under the conditions described in the materials and methods. The simultaneous rates obtained during nitrofurazone reduction were 3.12 ± 0.06 μM.s^{-1}.mg of enzyme^{-1} for nitrofurazone and 5.76 ± 0.25 μM.s^{-1}.mg of enzyme^{-1} for NADPH this gives an estimate for the molar ratio of the reaction of approximately 2 moles NADPH oxidation per mole nitrofurazone reduction. Mass spectroscopy data obtained from a completed reaction carried out in ammonium bicarbonate gave a major peak at 184 Da (Supp. Fig. 1).

Structure of paAzoR1 binding nitrofurazone. The structure of paAzoR1 binding to nitrofurazone was solved at a resolution of 2.08 Å with final R_{free} and R_{work} values of 20.4% and 16.1% respectively and with good stereochemistry (Table 1). No significant conformational changes were observed between the structures of paAzoR1 bound to methyl red and paAzoR1 bound to nitrofurazone (RMSD on carbon α positions 0.23 Å). No significant movements of the amino acid side chains within the active site were observed when the structures were compared.

Clear positive difference density was visible for the nitrofurazone bound within the active site after a single round of refinement in PHENIX (Fig. 2A). Nitrofurazone was built into the density initially in one orientation, however upon further refinement it became clear there was density for nitrofurazone in two overlapping orientations.

Table 1 | Processing and refinement statistics for paAzoR1 binding nitrofurazone.

	paAzoR1 nitrofurazone
Space Group	$P3_121$
α, β, γ (°)	90, 90, 120
a, *b*, *c* (Å)	82.20, 82.20, 108.46
Processing Statistics	
Resolution Range (Å)	29.76-2.08
Unique reflections[a]	25,761 (1,794)
R_{merge}[a]	0.061 (0.766)
$<I/\sigma(I)>$[a]	18.6 (2.0)
Completeness %[a]	99.6 (95.3)
Multiplicity [a]	5.4 (5.2)
Refinement Statistics	
R_{work} %	16.07
R_{free} %	20.35
RMS bond angle (°)	0.98
RMS bond length (Å)	0.007

[a]Numbers in parentheses are for the highest resolution shell.

In both orientations the nitro group of nitrofurazone is positioned above the N5 of FMN in contrast to the orientation observed in the structure of NfsB bound to nitrofurazone where the nitro is 7.7 Å from the N5 (Fig. 3F[11]). Nitrofurazone binds in an overlapping conformation to that previously observed for balsalazide bound to paAzoR1 (Fig. 2B[13]) and methyl red bound to the Y131F mutant of paAzoR1,[14] as a result it makes many of the same interactions. The furan rings of both conformers overlap the salicylate ring of balsalazide in the corresponding structure and the polar tail of nitrofurazone overlaps with the position of the azo bond of balsalazide as well as partially overlapping the 4-aminobenzoyl-β-alanine ring of balsalazide (Fig. 2B). As the furan ring forms weaker π−π stacking interactions, than the benzene rings of balsalazide, the furan ring binds at an angle to the plane of the FMN. As well as forming π-π stacking interactions with FMN, nitrofurazone forms hydrophobic interactions with Tyr131, Phe100, Phe151 and Phe173, while the nitro group points into a water filled channel close to the side chain of Asn99.

Discussion

paAzoR1 binds nitrofurazone with a significantly lower K_m than azo compounds[14] while the rate of reduction is also lower. The slow rate of reduction is likely to be due to competition between nitrofurazone and NADPH for binding to the active site. Due to the very high K_m of NADPH (~1.2 mM[14]) the tight binding of nitrofurazone causes substrate inhibition. Apparent V_{max} is higher than that previously observed in *R. sphaeroides* azoreductases (0.23 μM.s^{-1}.mg of enzyme^{-1}).[16] The rate of nitroreduction by paAzoR1 is significantly slower than in nitroreductases such as NfsB (k_{cat} 2.3 s^{-1} for paAzoR1 compared to 225 s^{-1} for NfsB[11]) suggesting that in bacteria the majority of activation is carried out by nitroreductases.

The calculated molar ratio of approximately 2:1 for the rate of NADPH oxidation to nitrofurazone reduction is in-line with the data that were obtained from Electrospray ionisation, time of flight mass spectroscopy (ESI-TOF-MS Sup. Fig. 1B). The mass spectroscopy data agree with previously published data[11] that show the final reaction product is consistent with the hydroxylamine reductive metabolite of nitrofurazone (MW = 184 Da).

As when determining the mechanism of reduction of azo drugs,[13] the tautomeric state of nitrofurazone bound to the enzyme is important, the tautomer that binds paAzoR1 can be determined from the structure. Nitrofurazone can exist in two tautomers (Fig. 1) that are broadly equivalent to the azo and hydrazo tautomers of balsalazide. Based on previous work on this enzyme, one might expect that the azo form would be the more likely substrate as it has a more quinone-like ring.[13] The azo form of the compound would be planar due to its extensive conjugated system, the density for nitrofurazone in the structure however is not planar (Fig. 2A) and this is more in keeping with the hydrazo tautomer where one of the nitrogen atoms is sp^3 hybridised. This hypothesis is in agreement with the proposed conformation of the bound balsalazide with where the "azo" bond is in a similar conformation (Fig. 2B).

In the structure of NfsB binding to nitrofurazone,[11] nitrofurazone is observed to bind within the active site in a non-planar conformation (similar to that observed in the structure with paAzoR1) with its nitro group bound 7.7 Å from the N5 of FMN. In this structure nitrofurazone is anchored within the active site via a network of nine

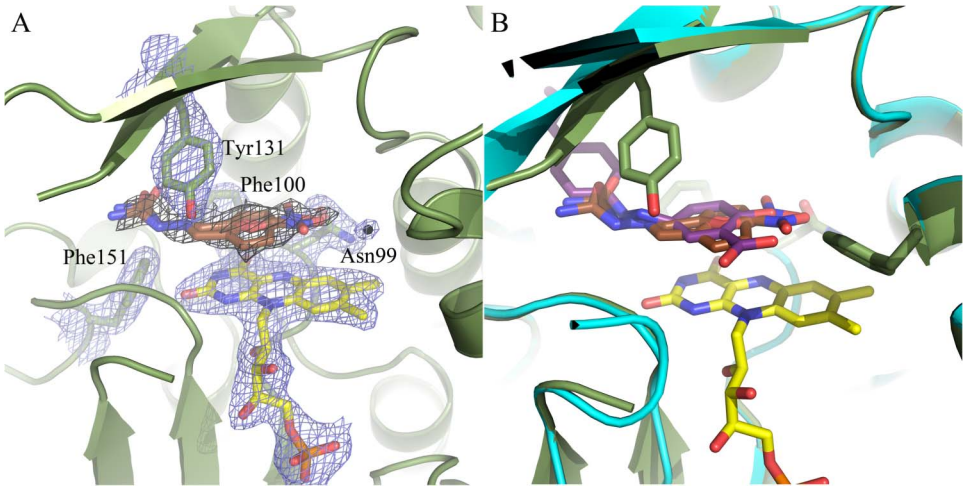

Figure 2 | Binding of nitrofurazone to paAzoR1. A) The binding of nitrofurazone in its two alternate conformers are shown with brown carbon atoms. The FMN is shown with yellow carbon atoms, both conformations of nitrofurazone are shown with brown carbon atoms. Important side chains are labelled. Blue mesh is the refined $2F_o$-F_c map contoured at 1σ, while black mesh is unbiased F_o-F_c map at 2.2σ. The black sphere represents a bound water molecule. (B) Comparison of balsalazide and nitrofurazone binding to paAzoR1. Colouring of nitrofurazone is as in (A) and balsalazide is in purple. This figure was produced in Pymol v1.1.[31]

short range hydrogen bonds to a combination of backbone amides, the ribose chain of FMN and the side chains of Glu165 and Asn71. This is in sharp contrast to the entirely hydrophobic interactions nitrofurazone makes within the active site of paAzoR1. As the binding conformation observed in the structure with NfsB is incompatible with the proposed mechanism of reduction it was speculated that when binding to the reduced enzyme, nitrofurazone binds in the reverse orientation, which would mean it is in a similar orientation to that observed in the paAzoR1-nitrofurazone strucuture. High resolution structural data (1.9 Å) from a closely related nitroreductase (88% identical – all active site residues are conserved) from *E. cloacae* in both the reduced and oxidised states show that reduction of FMN has little effect on surrounding active site residues.[17] Lower resolution (2.5 Å) structures of the reduced and oxidised forms of NfsB are also available and show there is no significant conformational changes in the active site residues as a result of FMN reduction.[18] It is therefore unlikely that reduced NfsB would bind nitrofurazone in a different conformation. The large number of interactions which are involved with the positioning of nitrofurazone in the conformation observed in the oxidised NfsB structure would

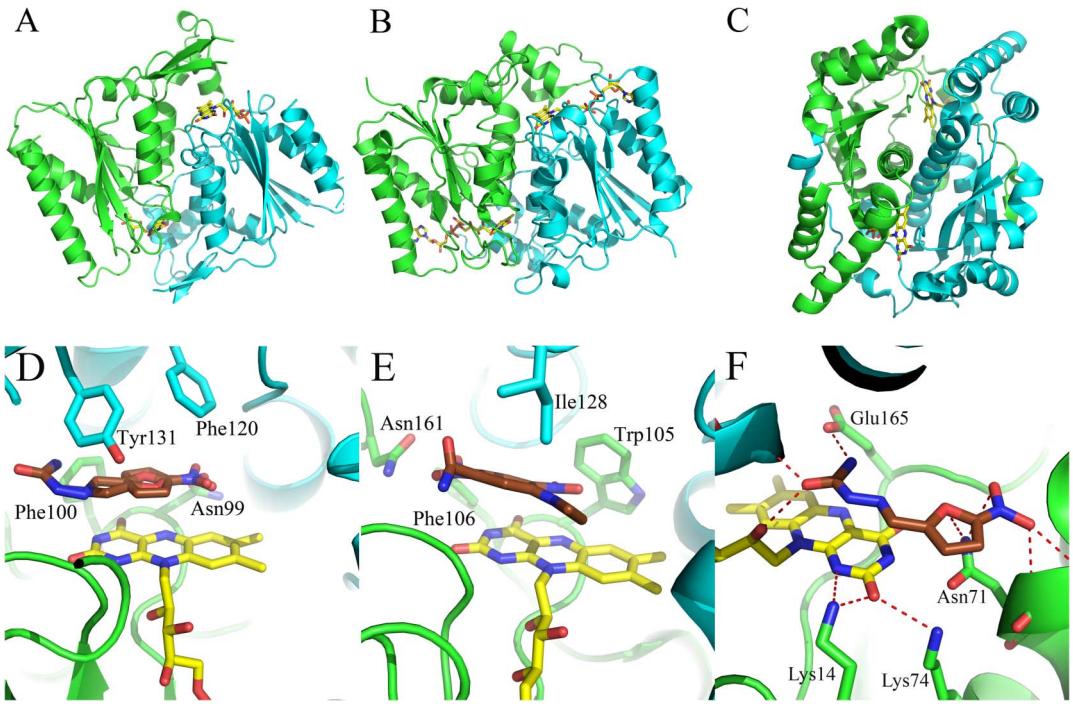

Figure 3 | Comparison of the overall structures (A–C) and nitroaromatic binding (D–F) of paAzoR1 (A,D), hNQO2 (B,E) and NfsB (C,F). (A–C) The overall structure of the dimeric forms of each of the three proteins. In all three panels monomer A is in green and B is in turquoise. (D–F) A detailed view of nitroaromatic drug binding within the active site of the enzymes (nitrofurazone in paAzoR1 and NfsB and CB1954 in hNQO2). In all panels the flavin cofactor is in yellow (FMN for paAzoR1 and NfsB, FAD for hNQO2). The Nitroaromatic drug is in brown in panels D–F. The structure of hNQO2 bound to CB1954 is from PDB 1XI2[20] and the structure of NfsB bound to nitrofurazone is from PDB 1YKI.[11]

mean that most likely alternate conformations will be energetically less favourable.

The proposed mechanism for nitroreduction, based on the azo tautomer being reduced, is shown in Fig. 4. Reduction reactions carried out by azoreductases proceed via a Bi-Bi ping-pong mechanism[1, 14] therefore as occurs during azoreduction,[13] substrate binding is preceded by NADPH binding. While bound to paAzoR1, NADPH transfers a hydride ion to the N5 of FMN which becomes $FMNH^-$. NADPH is subsequently displaced by nitrofurazone which accepts the hydride from $FMNH^-$ (Fig. 4A). The position of the nitrogen of the nitro group of each conformer of nitrofurazone within 3.6 Å of the N5 atom of FMN suggests that this is the target for hydride transfer. As the nitrogen atom of a nitro group is positively charged this also makes it a good candidate for transfer of the negatively charged hydride. To complete the reduction reaction a proton is accepted from the water molecule (Fig. 4A) which is stably bound to the protein within 3 Å of the nitro group of nitrofurazone (Fig. 2A). The reduction takes place twice according to the same mechanism, in order to get complete formation of the hydroxylamine species, therefore, a double Bi-Bi ping pong mechanism can also be proposed for nitrofurazone reduction in paAzoR1.

In addition it was noted that in the structure of paAzoR1 binding balsalazide, the oxygen of the quinoneimine tautomer of balsalazide is ~2.7 Å from the ketone of the Asn99 side chain. In the structure of paAzoR1 binding nitrofurazone one of the oxygen atoms of the nitro group is a similar distance from the carbonyl of Asn99. This positioning would allow hydrogen bond formation after reduction of either substrate which may help to stabilise the reduced form of the compound and thus may facilitate hydride transfer.

Nitrofurazone is known to be carcinogenic in mammals.[19] Unlike bacteria, humans have no homologues of NfsA and NfsB, as a result the majority of nitrofurazone activation in humans is proposed to occur via azoreductase-like enzymes. Humans have two azoreductase homologues, NAD(P)H quinone oxidorductase (hNQO) 1 and 2. Although bacterial azoreductases share minimal sequence similarity with hNQO1 and hNQO2[13] they are structurally related (Fig. 3A and B[20, 21]) and carry out many of the same reactions.[3] Both hNQO1 and hNQO2 have been shown to activate the anti-tumour pro-drug CB1954 via nitroreduction.[10] Activation of nitrofurazone by these enzymes may result in the carcinogenic properties in mammals and may be the cause of contact dermatitis experienced with nitrofurazone. The structure of hNQO2 binding CB1954 (Fig. 3E – PDB: 1XI2[20]) shows the nitro group that is reduced, binds with the nitrogen within 3.6 Å of the N5 of FMN in a similar position to the nitro group of nitrofurazone bound to paAzoR1. As a result it is proposed that other nitroaromatics are reduced by azoreductases via the same mechanism as is described here for nitrofurazone.

Methods

All reagents were obtained from Sigma-Aldrich (Poole, UK) unless otherwise specified.

Enzymology. Recombinant paAzoR1 was prepared as described previously.[2] Unless otherwise stated assays were carried out in 96-well format in a reaction volume of 100 µL using a Fluostar Omega plate reader from BMG labtech (Aylesbury, UK) typically using 10 µg paAzoR1 per well, 750 µM NADPH and varying concentrations of nitrofurazone in 20 mM Tris-HCl pH 8.0, 100 mM NaCl.

In order to estimate the stoichiometry of the enzymatic reduction of nitrofurazone by paAzoR1, the following reaction was carried out: 50 µM nitrofurazone, 400 µM NADPH, 10 µg paAzoR1. Both the oxidation of NADPH and the reduction of nitrofurazone were simultaneously followed spectrophotometrically at 340 nm and 405 nm respectively. The molar extinction coefficient of each species was determined at each λ_{max} ($\varepsilon_{NADPH,\ 340}$ 3,300 $M^{-1}cm^{-1}$, $\varepsilon_{NADPH,\ 405}$ 0 $M^{-1}cm^{-1}$, $\varepsilon_{Nitrofurazone,\ 405}$ 10,800 $M^{-1}cm^{-1}$ and $\varepsilon_{Nitrofurazone,\ 340}$ 9,500 $M^{-1}cm^{-1}$). Initial velocities were estimated via the following equations:

$$equation\ (1)\quad v_{i\,(340\ nm)} = \frac{\partial OD_{(340\ nm)}}{\partial t} = \ell \cdot \left(\frac{\partial [NADPH]}{\partial t} \varepsilon_{NADPH,\ 340} + \frac{\partial [nitrofuraz\ one]}{\partial t} \varepsilon_{nitrofuraz\ one,\ 340} \right)$$

$$equation\ (2)\quad v_{i\,(405\ nm)} = \frac{\partial OD_{(405\ nm)}}{\partial t} = \ell \cdot \left(\frac{\partial [nitrofuraz\ one]}{\partial t} \varepsilon_{nitrofuraz\ one,\ 405} \right)$$

As $\varepsilon_{NADPH\ 405}$ is 0, it is straightforward to determine the rate of nitrofurazone reduction $\frac{\partial [nitrofurazone]}{\partial t}$. This value is used to estimate $\frac{\partial [NADPH]}{\partial t}$ in equation (1). The ratio of $\frac{\partial [NADPH]}{\partial t}$ to $\frac{\partial [nitrofurazone]}{\partial t}$ provides an estimate for the ratio of NADPH oxidation to nitrofurazone reduction.

Identification of the products of nitrofurazone reduction. Identification of the final reduction products was carried out via ESI-TOF-MS. The reduced nitrofurazone was produced via the following reaction: 25 µM nitrofurazone, 0.5 mM NADPH and 100 µg paAzoR1 in a final volume of 1 mL containing 25 mM ammonium bicarbonate pH 7.9 (<0.5 mM NaCl). The reaction was monitored at OD_{405} on a Hitachi (Mannheim, Germany) U-2001 spectrophotometer and allowed to proceed to >98% completion. paAzoR1 was removed via a Sartorius (Ashtead, UK) 3 kDa molecular weight cutoff vivaspin centrifugal concentrator. The reaction mixture containing reduced nitrofurazone was lyophilised with a Lab mode (Milton Keynes, UK) ScanVac, before resuspension in 1 mL methanol. ESI-TOF-MS was carried out on a Waters (Elstree, UK) micromass mass spectrometer in negative ion mode.

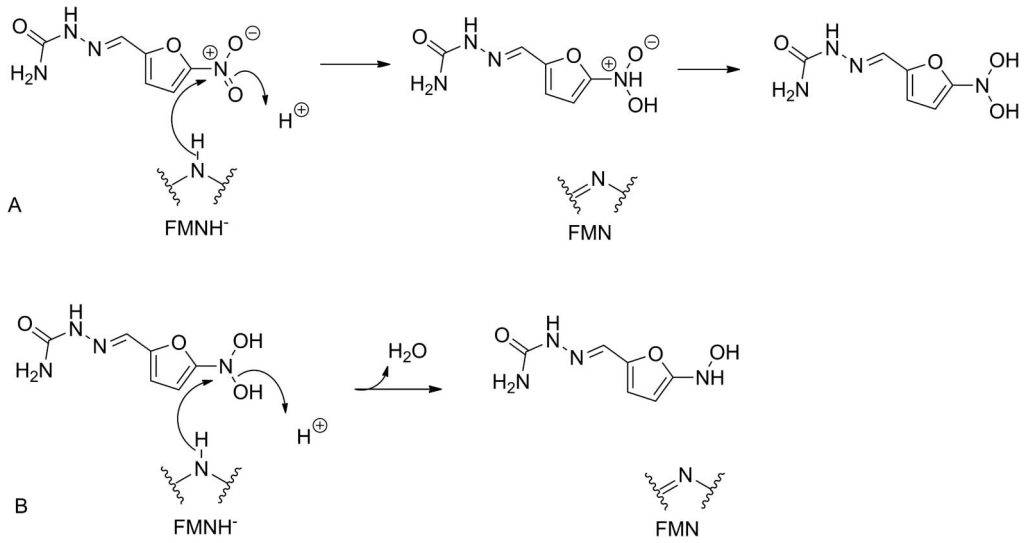

Figure 4 | Mechanism for nitrofurazone reduction. (A) First round of nitrofurazone reduction. (B) Second round of nitrofurazone reduction resulting in hydroxylamine formation. The proton in both (A) and (B) is likely to be donated by a stably bound water molecule observed in the structure (Fig. 2A). Before (A) and between (A) and (B) NADPH binds to paAzoR1 and transfers a hydride to FMN before being replaced by nitrofurazone.

Structure determination. paAzoR1 was mixed with nitrofurazone to give a protein solution of 23 $mg.mL^{-1}$ paAzoR1 in 20 mM Tris-HCl pH 8.0 with 2 mM nitrofurazone and incubated for an hour before being washed with 20 mM Tris-HCl pH 8.0 to remove DMSO. Crystals grew isomorphously under the same conditions as previously described,[2] briefly 2 μL protein complex was mixed with 2 μL 1.6 M $(NH_4)_2SO_4$ 0.1 M HEPES pH 7.5 in sitting drop format. Data for paAzoR1-nitrofurazone were collected at beamline I02 at the Diamond Light Source (Oxon, UK) with a Quantum ADSC detector. Data were integrated via XDS,[22] and scaled and merged with SCALA[23] both were run as part of xia2.[24] The structure was solved with the program PHASER,[25] using the structure of paAzoR1 stripped of its ligands (PDB: 2V9C[2]) as the search model. The atomic model was rebuilt and refined with Coot,[26] Refmac 5.5[27] and PHENIX.[28] Initial translation, libration and screw (TLS) parameters were determined with the program TLSMD[29] and TLS refinement was performed with PHENIX. Restraints for nitrofurazone were generated in eLBOW. Water molecules were added with PHENIX and Coot. The final model was validated via MolProbity[30] and all residues were shown to lie within the allowed regions of the Ramachandran plot (97.8% in the preferred region and 2.2% in the allowed region). Data collection and refinement statistics are shown in table 1. The structure was deposited in the protein data bank (PDB ID: 3R6W).

1. Nakanishi, M., Yatome, C., Ishida, N. & Kitade, Y. Putative ACP phosphodiesterase gene (acpD) encodes an azoreductase. *J Biol Chem* **276**, 46394–46399 (2001).
2. Wang, C. J. *et al.* Molecular cloning, characterisation and ligand-bound structure of an azoreductase from Pseudomonas aeruginosa. *J Mol Biol* **373**, 1213–1228 (2007).
3. Cui, K., Lu, A. Y. & Yang, C. S. Subunit functional studies of NAD(P)H:quinone oxidoreductase with a heterodimer approach. *Proc Natl Acad Sci U S A* **92**, 1043–1047 (1995).
4. Peppercorn, M. A. & Goldman, P. The role of intestinal bacteria in the metabolism of salicylazosulfapyridine. *J Pharmacol Exp Ther* **181**, 555–562 (1972).
5. Ryan, A., Wang, C. J., Laurieri, N., Westwood, I. & Sim, E. Reaction mechanism of azoreductases suggests convergent evolution with quinone oxidoreductases. *Protein Cell* **1**, 780–790 (2010).
6. Prosser, G. A. *et al.* Discovery and evaluation of Escherichia coli nitroreductases that activate the anti-cancer prodrug CB1954. *Biochemical Pharmacology* **79**, 678–687 (2010).
7. Boelsterli, U. A., Ho, H. K., Zhou, S. & Leow, K. Y. Bioactivation and hepatotoxicity of nitroaromatic drugs. *Curr Drug Metab* **7**, 715–727 (2006).
8. Tangallapally, R. P., Yendapally, R., Daniels, A. J. & Lee, R. E. Nitrofurans as Novel Anti-tuberculosis Agents: Identification, Development and Evaluation. *Current Topics in Medicinal Chemistry* **7**, 509–526 (2007).
9. Whiteway, J. *et al.* Oxygen-insensitive nitroreductases: analysis of the roles of nfsA and nfsB in development of resistance to 5-nitrofuran derivatives in Escherichia coli. *J Bacteriol* **180**, 5529–5539 (1998).
10. Knox, R. J. *et al.* Bioactivation of 5-(aziridin-1-yl)-2,4-dinitrobenzamide (CB 1954) by human NAD(P)H quinone oxidoreductase 2: a novel co-substrate-mediated antitumor prodrug therapy. *Cancer Res* **60**, 4179–4186 (2000).
11. Race, P. R. *et al.* Structural and mechanistic studies of Escherichia coli nitroreductase with the antibiotic nitrofurazone. Reversed binding orientations in different redox states of the enzyme. *J Biol Chem* **280**, 13256–13264 (2005).
12. Hiraku, Y. *et al.* Mechanism of carcinogenesis induced by a veterinary antimicrobial drug, nitrofurazone, via oxidative DNA damage and cell proliferation. *Cancer Lett* **215**, 141–150 (2004).
13. Ryan, A. *et al.* A novel mechanism for azoreduction. *J Mol Biol* **400**, 24–37 (2010).
14. Wang, C. J. *et al.* Role of Tyrosine 131 in the active site of paAzoR1, an azoreductase with specificity for the inflammatory bowel disease pro-drug balsalazide. *Acta Crystallogr F Struct Biol Cryst Commun* **66**, 2–7 (2010).
15. Liger, D. *et al.* Crystal structure and functional characterization of yeast YLR011wp, an enzyme with NAD(P)H-FMN and ferric iron reductase activities. *J. Biol. Chem.* **279**, 34890–34897 (2004).
16. Liu, G. *et al.* Site-directed mutagenesis of substrate binding sites of azoreductase from Rhodobacter sphaeroides. *Biotechnol Lett* **30**, 869–875 (2008).
17. Haynes, C. A., Koder, R. L., Miller, A. F. & Rodgers, D. W. Structures of nitroreductase in three states: effects of inhibitor binding and reduction. *J Biol Chem* **277**, 11513–11520 (2002).
18. Johansson, E., Parkinson, G. N., Denny, W. A. & Neidle, S. Studies on the nitroreductase prodrug-activating system. Crystal structures of complexes with the inhibitor dicoumarol and dinitrobenzamide prodrugs and of the enzyme active form. *J Med Chem* **46**, 4009–4020 (2003).
19. Kari, F. NTP Toxicology and Carcinogenesis Studies of Nitrofurazone (CAS No.59-87-0) in F344/N Rats and B6C3F1 Mice (Feed Studies). *Natl Toxicol Program Tech Rep Ser* **337**, 1–183 (1988).
20. Fu, Y., Buryanovskyy, L. & Zhang, Z. Crystal structure of quinone reductase 2 in complex with cancer prodrug CB1954. *Biochem Biophys Res Commun* **336**, 332–338 (2005).
21. Li, R., Bianchet, M. A., Talalay, P. & Amzel, L. M. The three-dimensional structure of NAD(P)H:quinone reductase, a flavoprotein involved in cancer chemoprotection and chemotherapy: mechanism of the two-electron reduction. *Proc Natl Acad Sci U S A* **92**, 8846–8850 (1995).
22. Kabsch, W. XDS. *Acta Crystallographica Section D* **66**, 125–132 (2010).
23. Bailey, S. The CCP4 suit – programs for protein crystallography. *Acta Crystallogr D Biol Crystallogr* **58**, 760–763 (1994).
24. Winter, G. xia2: an expert system for macromolecular crystallography data reduction. *J Appl Crystallogr* **43**, 186–190 (2010).
25. McCoy, A. J. *et al.* Phaser crystallographic software. *J Appl Crystallogr* **40**, 658–674 (2007).
26. Emsley, P., Lohkamp, B., Scott, W. G. & Cowtan, K. Features and development of Coot. *Acta Crystallogr D Biol Crystallogr* **66**, 486–501 (2010).
27. Murshudov, G. N., Vagin, A. A. & Dodson, E. J. Refinement of macromolecular structures by the maximum-likelihood method. *Acta Crystallogr D Biol Crystallogr* **53**, 240–255 (1997).
28. Adams, P. D. *et al.* PHENIX: a comprehensive Python-based system for macromolecular structure solution. *Acta Crystallogr D Biol Crystallogr* **66**, 213–221 (2010).
29. Painter, J. & Merritt, E. A. Optimal description of a protein structure in terms of multiple groups undergoing TLS motion. *Acta Crystallogr D Biol Crystallogr* **62**, 439–450 (2006).
30. Chen, V. B. *et al.* MolProbity: all-atom structure validation for macromolecular crystallography. *Acta Crystallogr D Biol Crystallogr* **66**, 12–21 (2010).
31. DeLano, W. L., Edn. Version 1.1 (DeLano Scientific, Palo Alto, , .CA, , USA; 2008).

Acknowledgments

We thank Dr. A. Russell for use of the Fluostar Omega plate reader, Dr J. Swinden for carrying out the ESI-TOF-MS experiments and Prof. J. Brown for useful discussions regarding the manuscript.

Author contributions

A. Ryan designed the experiments, carried out some of the experiments, carried out data analysis and wrote the manuscript. E. Kaplan carried out most of the experiments and data analysis. N. Laurieri was involved with planning of experiments as well as data analysis and contributed to writing of the manuscript. E. Lowe carried out crystallographic data collection and aided with data analysis. E. Sim coordinated the project as well as helping to write the manuscript.

Additional information

Supplementary Information accompanies this paper at http://www.nature.com/scientificreports

Competing Financial Interests: The authors declare that they hold no competing financial interests.

How to cite this article: Ryan A., Kaplan E., Laurieri N., Lowe E., & Sim E. Activation of nitrofurazone by azoreductases: multiple activities in one enzyme. *Sci. Rep.* **1**, 63; DOI:10.1038/srep00063 (2011).